Robust error metrics for adaptivity with ray-effects

Steven Dargaville

Richard Smedley-Stevenson, Paul Smith, Christopher Pain

Applied Modelling and Computation Group, Imperial College London

4th November 2020

Ray-effects

- Any non-rotational invariant (NRI) angular discretisation gives ray-effects (Sn, FEM, etc)
- This is the pre-asymptotic region of convergence
- Want to solve problems with small solid angle (1×10^{-9} sr.)

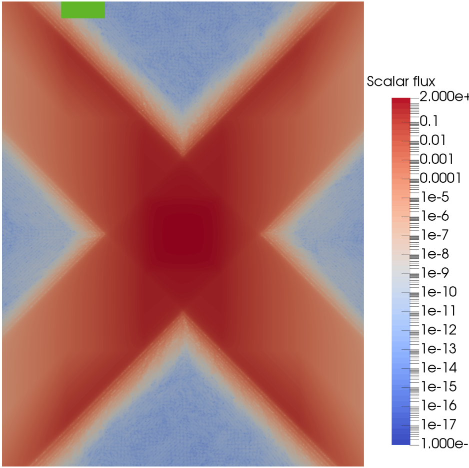

Angular adaptivity

- Often don't need high resolution everywhere in space/energy
- Error metric must:

1. Be able to refine in the pre-asymptotic regime to "resolve" ray-effects
2. Be able to refine in asymptotic regime to capture real discontinuities
3. Be locally refineable
4. Be scalably refineable

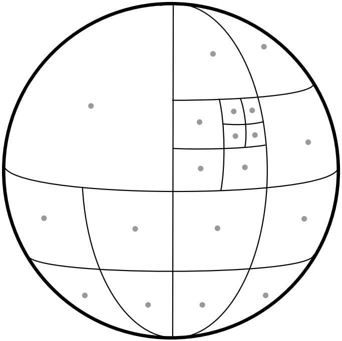

Haar wavelets

- Hierarchical basis on each octant P^0 DG
- Hence equivalent to P^0 DG FEM in angle
- Can do arbitrary anisotropic refinement in $\mathcal{O}(n)$

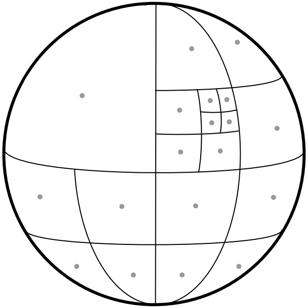

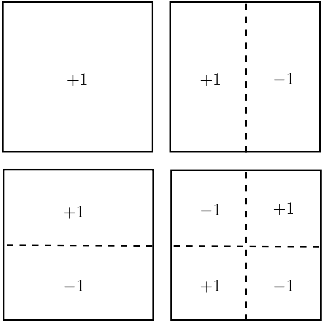

S. Dargaville, A. G. Buchan, R. P. Smedley-Stevenson, P. N. Smith, and C. C. Pain. Scalable angular adaptivity for Boltzmann transport. *Journal of Computational Physics*, 406(109124), 2020a

Error metrics

- Could use regular error metric
- Rely on wavelet properties (norm-equiv and cancellation)
- Hence refine where flux is big and discontinuous

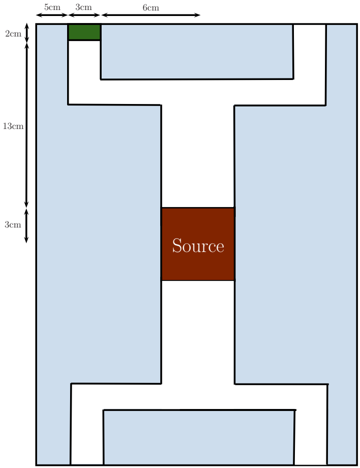

Figure: The red region is a source, the blue region is pure absorber (1 cm^{-1}), with the white, green and red regions pure vacuum.

Regular adapt + load balance

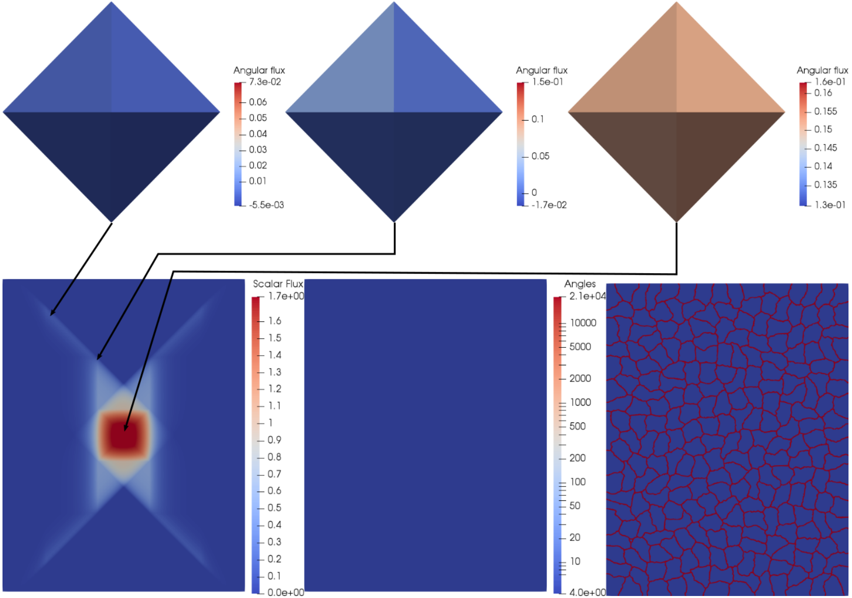

Goal-based error metric

- Chose a goal to reduce error in (e.g., avg flux in region)
- Solve forward and adjoint problems - $\mathbf{\Psi}$ and $\mathbf{\Psi}^*$
- Form forward and adjoint residuals - $\hat{\mathbf{R}}$ and $\hat{\mathbf{R}}^*$
- Dual-weighted residual method gives:

$$\mathbf{e} = \frac{\max\{|\mathbf{\Psi} \odot \hat{\mathbf{R}}^*|, |\mathbf{\Psi}^* \odot \hat{\mathbf{R}}|\} N_{\mathrm{DOF}}}{\tau},$$

- Then trigger refinement where $\mathbf{e}$ is big

Goal-based adaptivity and ray-effects

- Rely on being able to "see" the detector in pre-asymptotic
- Error metric is zero - no adapt!
- Easy to not bump into this

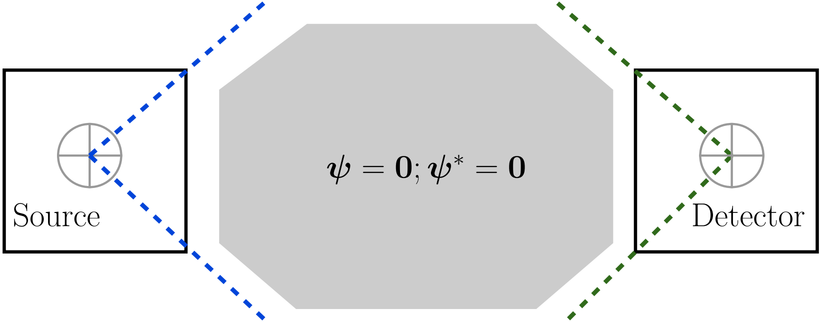

Figure: Source/detctor problem in a vacuum

"Fake" robustness

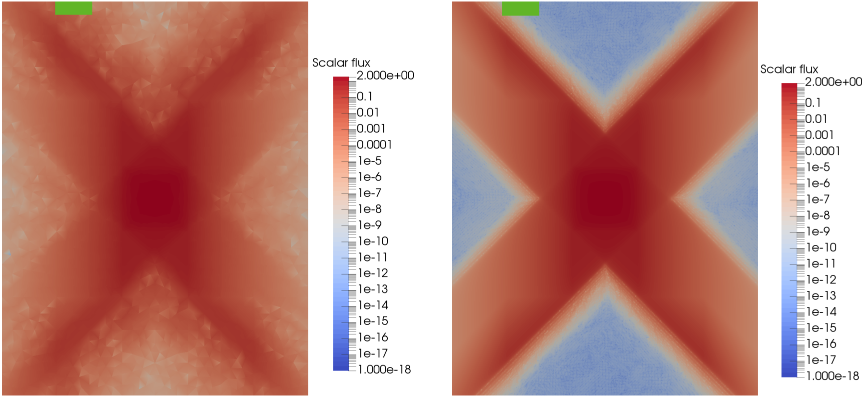

Figure: H_1 solution on coarse (3000 elements) and fine mesh (265k elements)

- Detector response on coarse mesh from numerical diffusion
- Refined spatial mesh gives zero response
- "Fake" response also from aligned detector, or scatter path

Robust error metric

- Let's try and build a cheap surrogate solution without ray-effects
- Use this to trigger refinement in pre-asymptotic
- Can't use diffusion equation as isotropic in angle
- Can't use different quadrature/NRI disc.
- Could add angular diffusion to NRI but how to add "enough"/"not too much"
- P_n is rotationally invariant but poorly conditioned due to Gibbs with streaming

Robustness with FP_n

- Filtered P_n equivalent to adding angular diffusion
- Converges to true transport solution
- No-ray effects and constant condition number with pure streaming
- But $\mathcal{O}(n^2)$ because of BCs

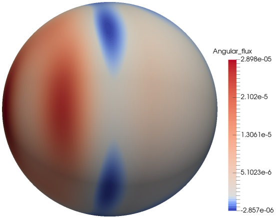

Figure: P_n solution

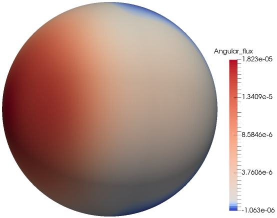

Figure: Filtered P_n solution

Ryan G. McClarren and Cory D. Hauck. Robust and accurate filtered spherical harmonics expansions for radiative transfer. *Journal of Computational Physics*, 229(16):5597–5614, August 2010. ISSN 0021-9991

S. Dargaville, A. G. Buchan, R. P. Smedley-Stevenson, P. N. Smith, and C. C. Pain. Angular adaptivity with spherical harmonics for Boltzmann transport. *Journal of Computational Physics*, 397(108846), 2019

Asymptotic regimes

- Exploit pre-asymptotic regime is different for FP$_n$ and NRI disc.
- Use low-order FP$_n$ $\mathcal{O}(n^2)$ solution to bootstrap our error metric
- Then scalable $\mathcal{O}(n)$ Haar adapt takes over

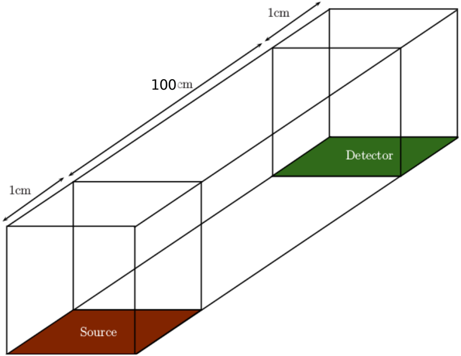

Figure: Pure vacuum source/detector

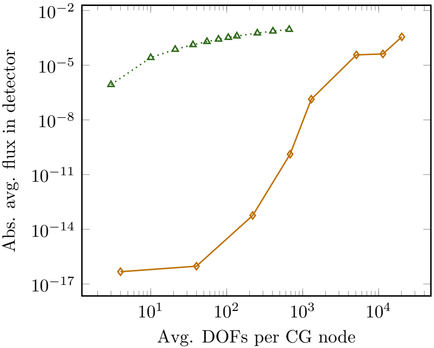

Figure: $\diamond$ uniform LS P^0 FEM, $\triangle$ is uniform FP$_n$ with $\Sigma_{\mathrm{f}} = 0.1$.

Simple heuristic

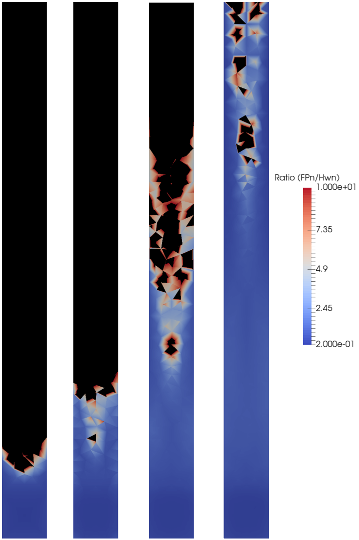

Figure: FP_1 vs Haar solution
Shaded black where > 10

- Solve Haar forward/adjoint, then FP_n forward/adjoint
- Use FP_n solution in metric if 10 times bigger than Haar
- Then refine Haars and repeat
- In limit of FP_n refined, heuristic reduced and τ reduced
- Goal-based Haar adapt converges to true solution

Duct problem - Goal based

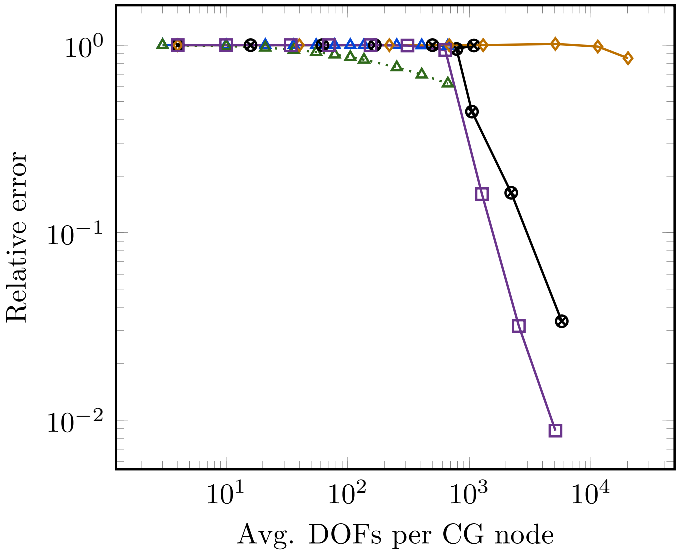

Figure: □ is fixed refined Haars, ⊗ goal-based Haar adapts, ◇ uniform LS P^0 FEM, △ is uniform FP_n with $\Sigma_f = 0.1$.

Duct problem - Goal based

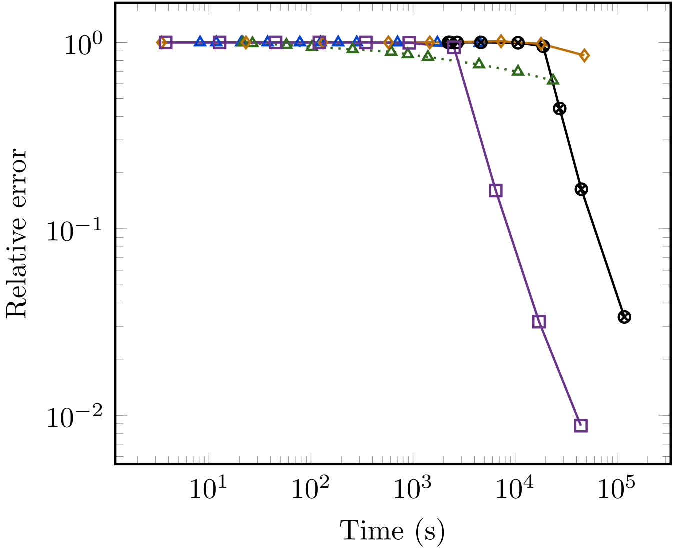

Figure: □ is fixed refined Haars, ⊗ goal-based Haar adapts, ◇ uniform LS P^0 FEM, △ is uniform FP_n with $\Sigma_f = 0.1$.

Duct problem - Goal based

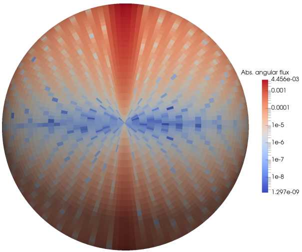

Figure: FP_{21} solution at midpoint

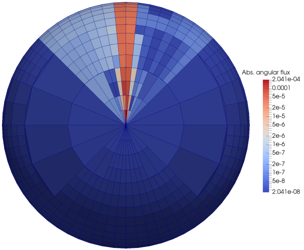

Figure: Haar adapt after 5 steps

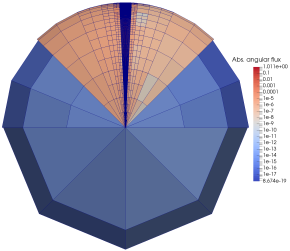

Figure: Haar adapt after 10 steps

3D scatter box

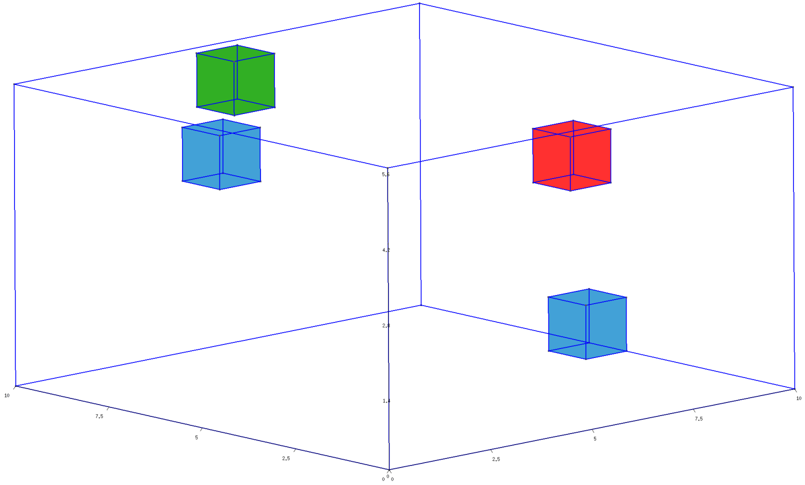

Figure: 10x10x6cm box, all regions vacuum except blue pure scattering regions (1cm^{-1}), red region is source, green region is detector.

3D scatter box - Goal based

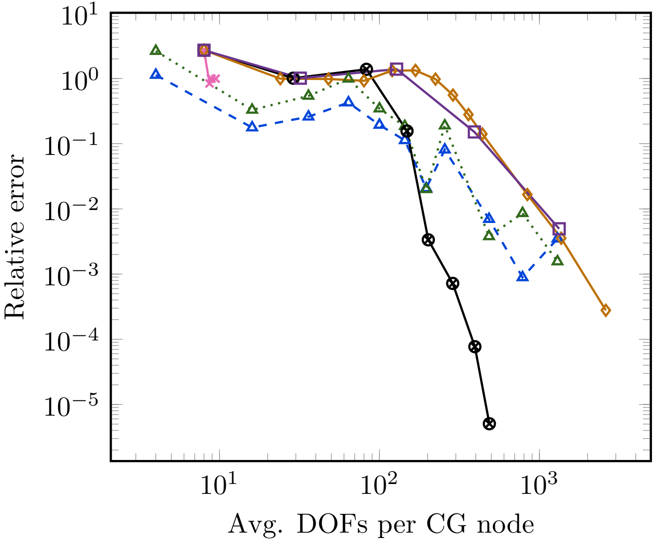

Figure: □ is fixed refined Haars, ⊗ goal-based Haar adapts, × non-robust Haar adapt, ◇ uniform LS P^0 FEM, △ is uniform FP_n with $\Sigma_\mathrm{f} = 0.1$.

3D scatter box - Goal based

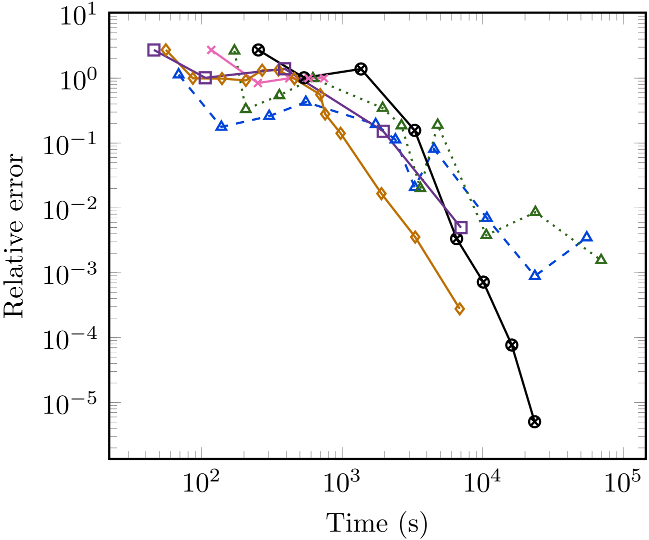

Figure: □ is fixed refined Haars, ⊗ goal-based Haar adapts, × non-robust Haar adapt, ◇ uniform LS P^0 FEM, △ is uniform FP_n with $\Sigma_f = 0.1$.

3D scatter box - Goal based

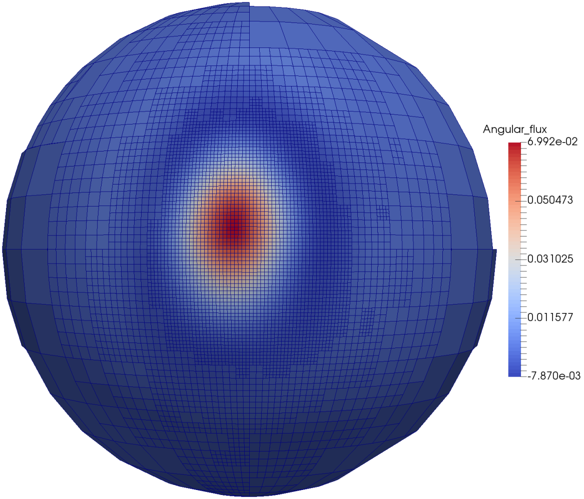

Figure: Adapted angular flux in direct path between source/detector.

Conclusions

- If you're doing goal-based space or angle adapts
- Be careful about the pre-asymptotic regime with streaming
- Using FP_n surrogate solution brings robustness
- If you aren't robust in all parameter regimes, why bother?
- Hopefully now robust for combined space + angle adapts

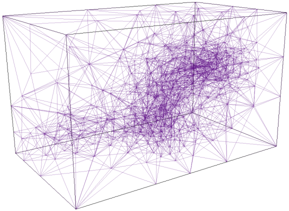

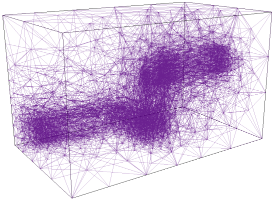

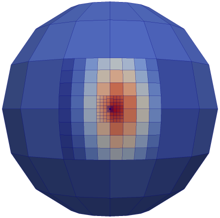

Thanks for listening

S. Dargaville, A. G. Buchan, R. P. Smedley-Stevenson, P. N. Smith, and C. C. Pain. Angular adaptivity with spherical harmonics for Boltzmann transport. *Journal of Computational Physics*, 397(108846), 2019

S. Dargaville, A. G. Buchan, R. P. Smedley-Stevenson, P. N. Smith, and C. C. Pain. Scalable angular adaptivity for Boltzmann transport. *Journal of Computational Physics*, 406(109124), 2020a

S. Dargaville, R. P. Smedley-Stevenson, P. N. Smith, and C. C. Pain. Goal-based angular adaptivity for boltzmann transport in the presence of ray-effects. *Journal of Computational Physics*, 421(109759), 2020b

Dogleg problem - Goal based

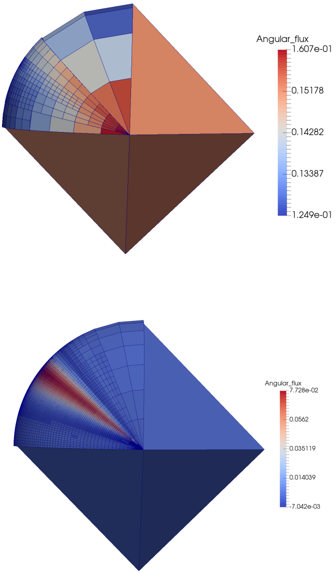

Figure: Flux near source and duct

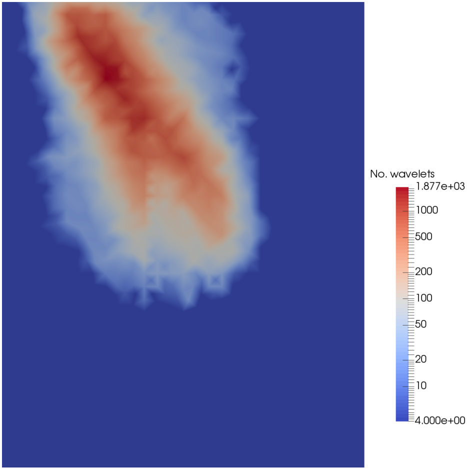

Figure: No. angles after 9 adapt steps

Dogleg problem - Goal based

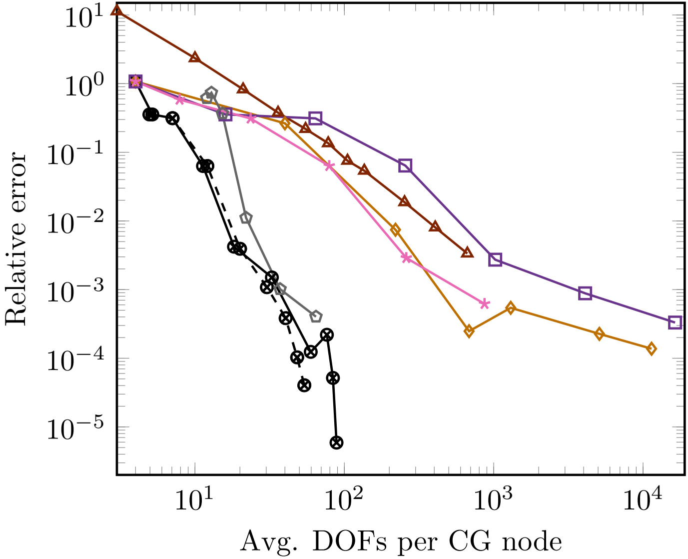

Figure: △ is uniform P_n, the □ is uniform Haars, * regular adapt Haars, ⬠ goal-based linear wavelets [1], ⊗ goal-based Haar adapts, ◇ uniform LS P^0 FEM

Dogleg problem - Goal based

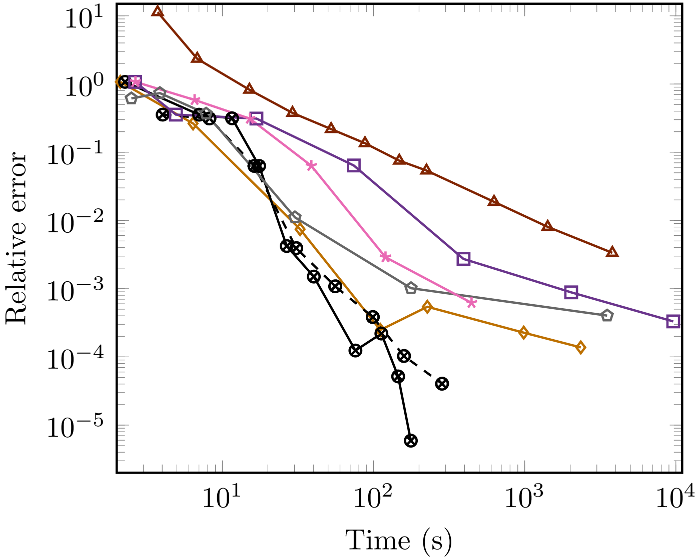

Figure: △ is uniform P_n, the □ is uniform Haars, * regular adapt Haars, ⬠ goal-based linear wavelets [1], ⊗ goal-based Haar adapts, ◇ uniform LS P^0 FEM

Dogleg problem - Goal based

Adapt step:	1	2	3	4	5
Cum. runtime (μs) per final DOF:	57	130	144	134	121
Peak memory use:	254.6	199.2	155.9	95.3	66.4

Adapt step:	6	7	8	9	10
Cum. runtime (μs) per final DOF:	97.2	94.6	102	119	136
Peak memory use:	48.8	35.2	31.3	30.72	30.67

Table: Time and peak memory in copies of adapted ang. flux

- Linear growth in memory consumption per adapted DOF
- Close to linear growth in runtime per adapted DOF
- We have scalability in this problem - min solid angle 5×10^{-6} sr
- Uniform DG LS S_{780} sweep would need 136 ns solve time per DOF

Ray-effect free

- We need something to "bootstrap" the angle adapt
- Or to compute an importance map/weight window in angle
- Diffusion approximation won't work - Constant in angle
- Can't use anything with ray-effects
- P_n doesn't have ray effects, but Gibbs
- Filtered P_n removes Gibbs, reduces convg. rate in smooth problems
- Still converges to real transport solution

S. Dargaville, A. G. Buchan, R. P. Smedley-Stevenson, P. N. Smith, and C. C. Pain. Angular adaptivity with spherical harmonics for Boltzmann transport. *Journal of Computational Physics*, 397(108846), 2019

Filtered P_n

$$f(\boldsymbol{\Omega}) = \sum_{l=0}^{N} \sum_{m=-l}^{l} \left[\sigma\left(\frac{l}{N+1}\right)\right]^{s} f_{l,m} Y_{l,m}(\boldsymbol{\Omega}),$$

- where $\sigma(\eta)$ is a filter function and s is a strength.
- Rotationally-invariant
- (Close to) constant condition number with angular refinement
- Equivalent to a forward-peaked scattering operator
- Filter acts like angular "diffusion"
- Still $\mathcal{O}(n^2)$ in angle size (BCs, jump terms)

Ryan G. McClarren and Cory D. Hauck. Robust and accurate filtered spherical harmonics expansions for radiative transfer. *Journal of Computational Physics*, 229(16):5597–5614, August 2010. ISSN 0021-9991

David Radice, Ernazar Abdikamalov, Luciano Rezzolla, and Christian D. Ott. A new spherical harmonics scheme for multi-dimensional radiation transport I. Static matter configurations. *Journal of Computational Physics*, 242:648–669, June 2013. ISSN 0021-9991. doi: 10.1016/j.jcp.2013.01.048. URL http://www.sciencedirect.com/science/article/pii/S0021999113001125

Filtered P_n

- Compute (low-order but ray-effect free) FP_n solution
- Use this to compute error metric/importance map
- Then scalable adapt or Monte-Carlo takes over and resolves to high accuracy

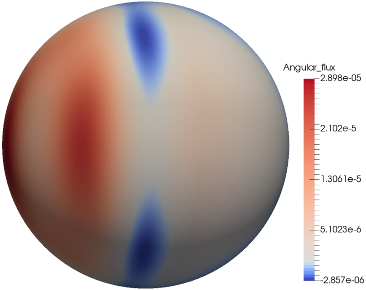

Figure: P_n solution

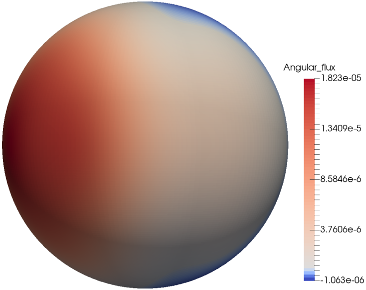

Figure: Filtered P_n solution

Adaptivity with FP$_n$

- FP$_n$ will be (at best) $\mathcal{O}(n^2)$ in angle size
- Angular adaptivity can reduce the size of n
- The filter smooths out Gibbs oscillations
- We only want to apply that heavily around discontinuities
- Our adaptivity process can tell us where there are discontinuities
- Preserves high order where smooth

Adaptivity with FP$_n$

- Fix constant filter strength Σ_{f}^{1}
- Solve coarse linear systems (forward + adjoint)
- Compute goal-based error metrics and refine
- Our spatial discretisation gives us the amount of stabilisation applied $\tilde{\Sigma}_{\mathrm{stab}}$
- Compute (heuristic) spatially-dependent filter strength Σ_{f}
- Solve refined/spatially-filtered linear system
- ...

$$\Sigma_{\mathrm{f}} = \Sigma_{\mathrm{f}}^{1} \left(\frac{|\tilde{\Sigma}_{\mathrm{stab}}|}{\max(|\tilde{\Sigma}_{\mathrm{stab}}|)} \right)^{(1/3)} .$$

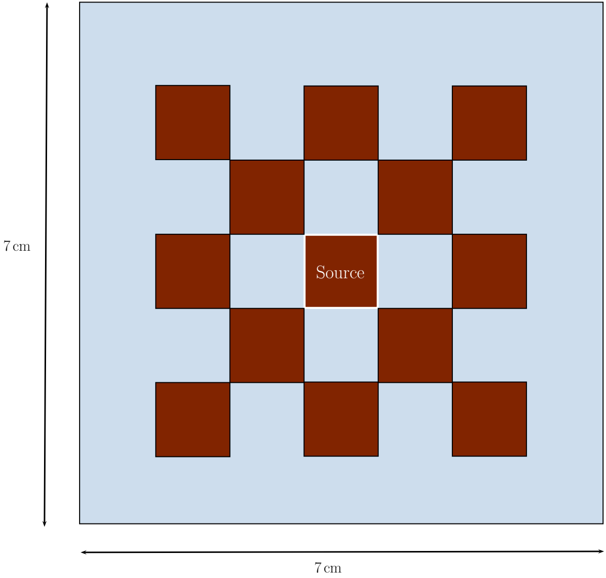

Figure: Schematic of the 2D Brunner lattice problem. The red region is a pure absorber (10 cm^{-1}), the blue region is pure scatter (1 cm^{-1}), with the the white bordered region a source.

Brunner problem with adapted FP_n

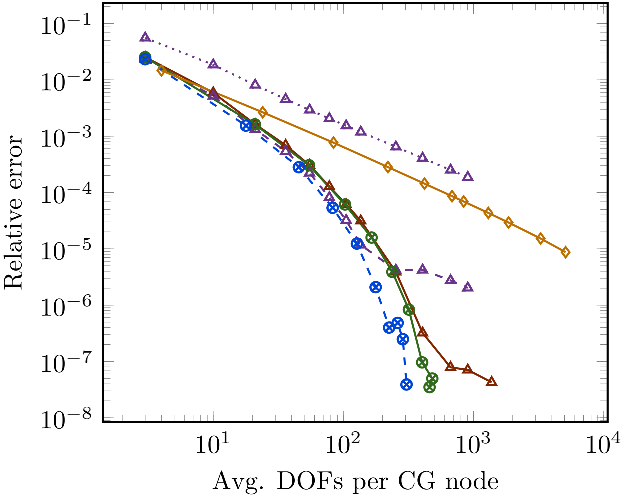

Figure: The ⊗ goal-based P_n adapts, dashed ⊗ goal-based FP_n adapts, spatially dependent Σ_f, with $\Sigma_\mathrm{f}^1 = 10$. Solid △ is uniform P_n, the dotted △ is uniform FP_n with $\Sigma_\mathrm{f} = 10$ with dashed $\Sigma_\mathrm{f} = 1$ and ◇ uniform LS P^0 FEM.

Brunner problem with adapted FP$_n$

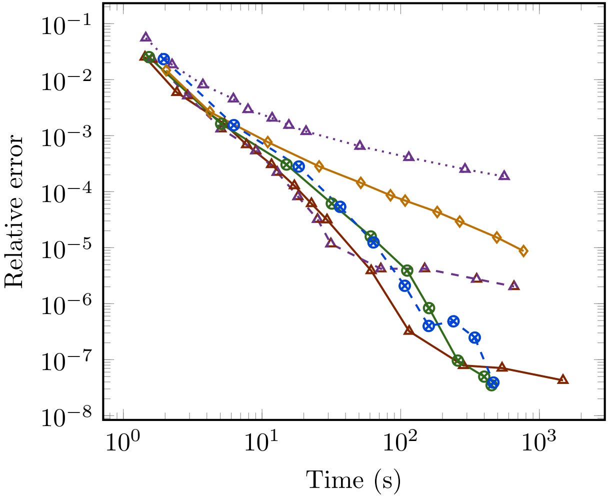

Figure: The ⊗ goal-based P$_n$ adapts, dashed ⊗ goal-based FP$_n$ adapts, spatially dependent Σ_f, with $\Sigma_\mathrm{f}^1 = 10$. Solid △ is uniform P$_n$, the dotted △ is uniform FP$_n$ with $\Sigma_\mathrm{f} = 10$ with dashed $\Sigma_\mathrm{f} = 1$ and ◇ uniform LS P^0 FEM.

Brunner problem with adapted FP$_n$

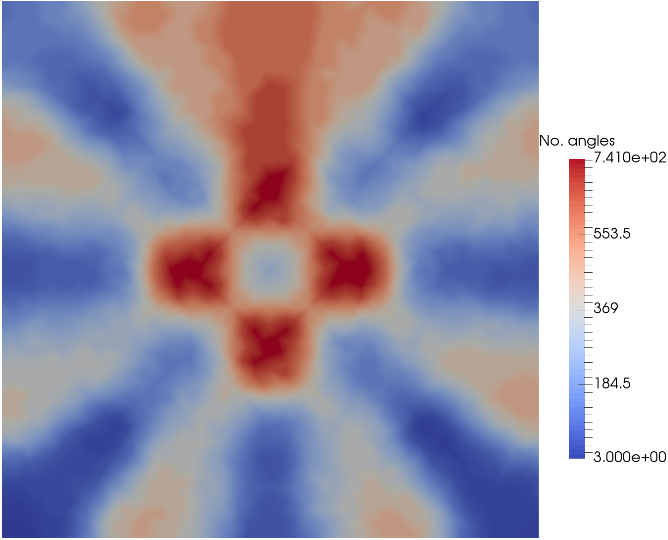

Figure: Number of angles applied by our adaptive FP$_n$ algorithm after 10 adapt steps.

Brunner problem with adapted FP$_n$

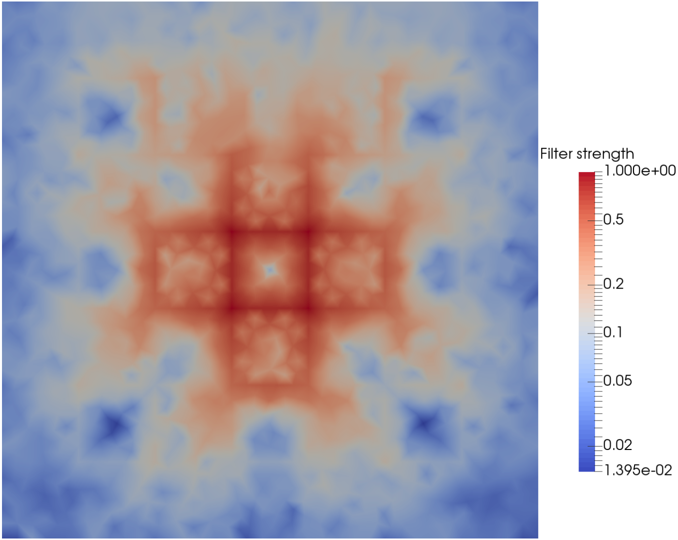

Figure: Spatially-dependent filter values after 10 adapt steps

Dogleg problem with adapted FP$_n$

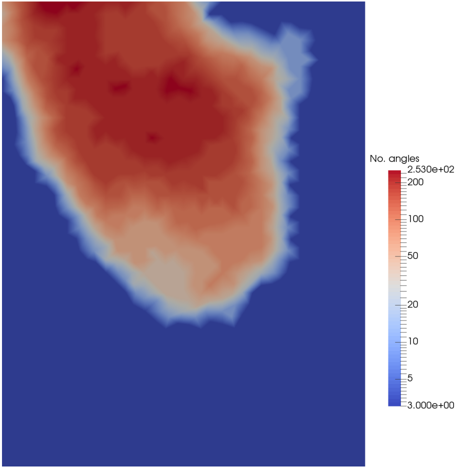

Figure: No angles after 10 adapt steps

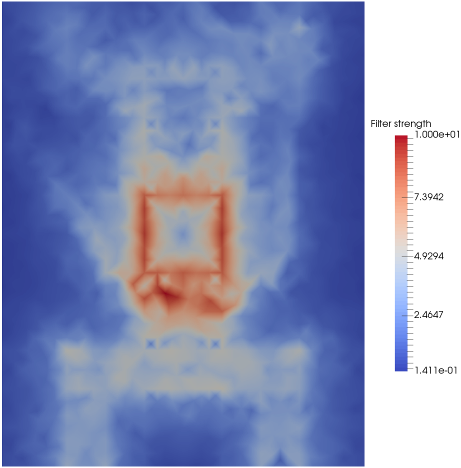

Figure: Filter strength

Dogleg problem with adapted FP_n

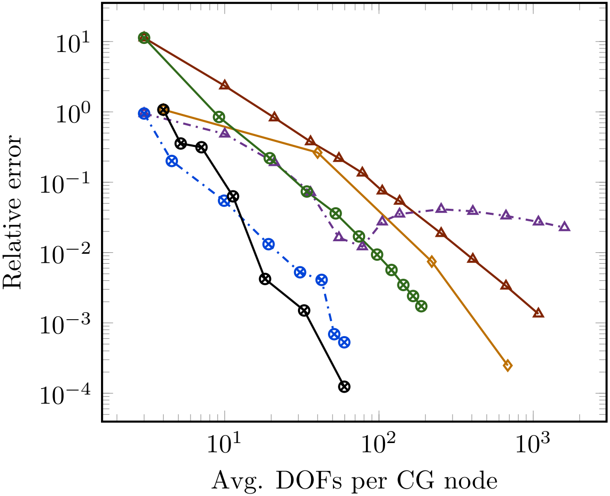

Figure: The $\otimes$ goal-based P_n adapts, dashed $\otimes$ goal-based FP_n adapts, spatially dependent Σ_f, with $\Sigma_f^1 = 10$. Solid $\triangle$ is uniform P_n, the dash-dotted $\triangle$ is uniform FP_n with $\Sigma_f = 10$ and $\diamond$ uniform LS P^0 FEM. The $\otimes$ are goal-based adapted non-standard Haar wavelets

Dogleg problem with adapted FP_n

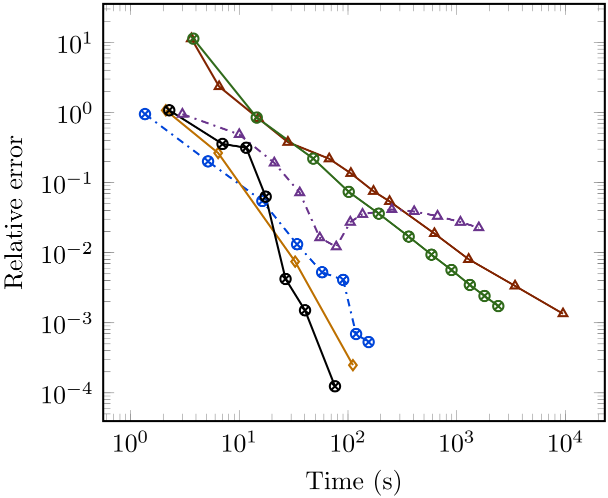

Figure: The $\otimes$ goal-based P_n adapts, dashed $\otimes$ goal-based FP_n adapts, spatially dependent Σ_f, with $\Sigma_\mathrm{f}^1 = 10$. Solid $\triangle$ is uniform P_n, the dash-dotted $\triangle$ is uniform FP_n with $\Sigma_\mathrm{f} = 10$ and $\diamond$ uniform LS P^0 FEM. The $\otimes$ are goal-based adapted non-standard Haar wavelets

Goal-based adaptivity

- We need something to "bootstrap" the adapt
- Diffusion approximation won't work - H_1 captures exactly
- P_n doesn't have ray effects, but Gibbs
- Filtered P_n removes Gibbs, reduces convg. rate to ~ 0.5
- Applying BCs and dense angular matrices still $\mathcal{O}(n^2)$
- Use (bad but ray-effect free) FP_n solution to force adapts
- When a single ray can see detector
- Then scalable adapt takes over and resolves to high accuracy
- Note "high accuracy" can mean 1 decimal place!

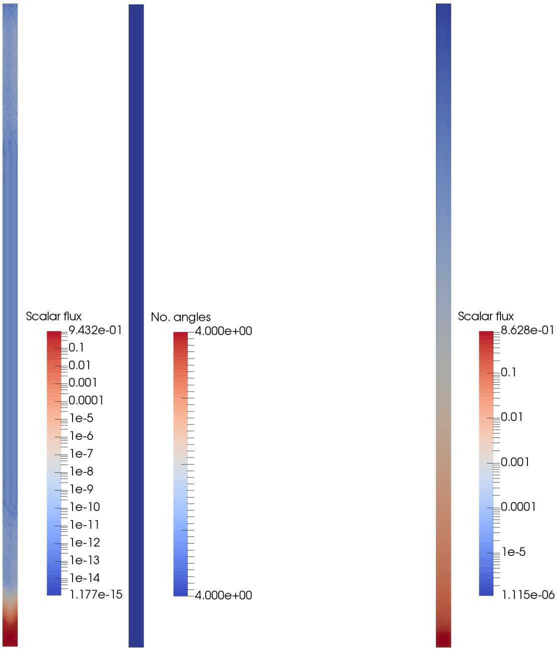

Figure: H_1 and FP_{15} in vacuum source/detector problem - 40/1 ratio

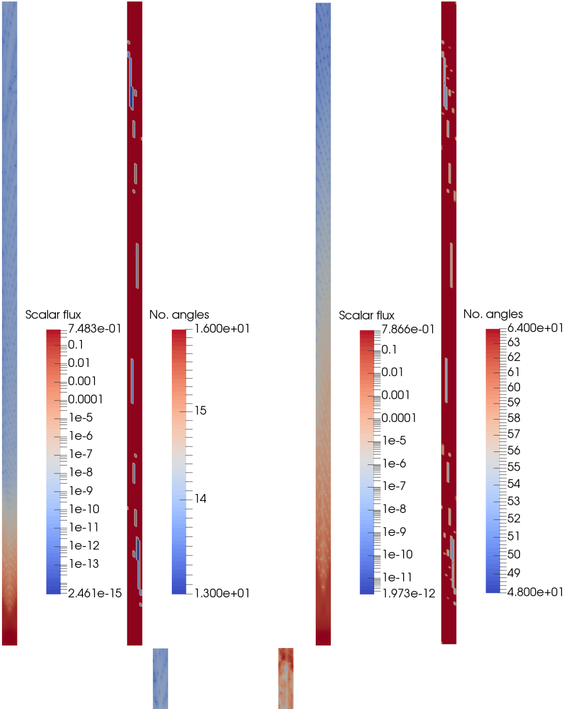
Scalar flux
7.483e-01
0.1
0.01
0.001
0.0001
1e-5
1e-6
1e-7
1e-8
1e-9
1e-10
1e-11
1e-12
1e-13
2.461e-15
No. angles
1.600e+01
15
14
1.300e+01
Scalar flux
7.866e-01
0.1
0.01
0.001
0.0001
1e-5
1e-6
1e-7
1e-8
1e-9
1e-10
1e-11
1.973e-12
No. angles
6.400e+01
63
62
61
60
59
58
57
56
55
54
53
52
51
50
49
4.800e+01

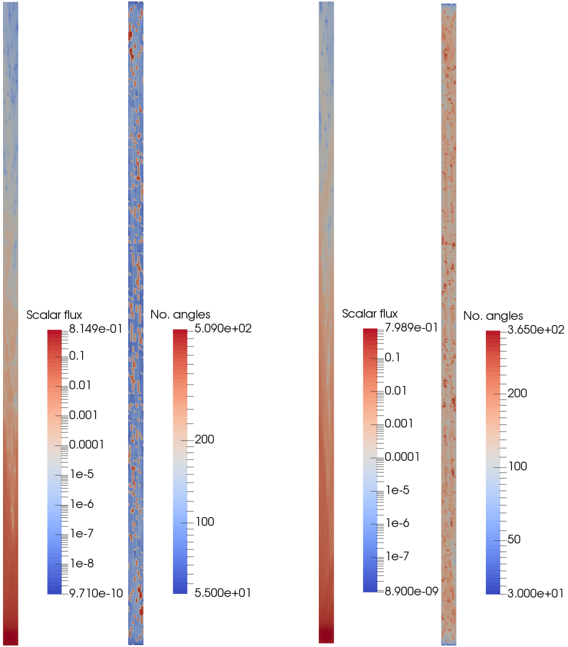
Scalar flux
8.149e-01
0.1
0.01
0.001
0.0001
1e-5
1e-6
1e-7
1e-8
9.710e-10
No. angles
5.090e+02
200
100
5.500e+01
Scalar flux
7.989e-01
0.1
0.01
0.001
0.0001
1e-5
1e-6
1e-7
8.900e-09
No. angles
3.650e+02
200
100
50
3.000e+01

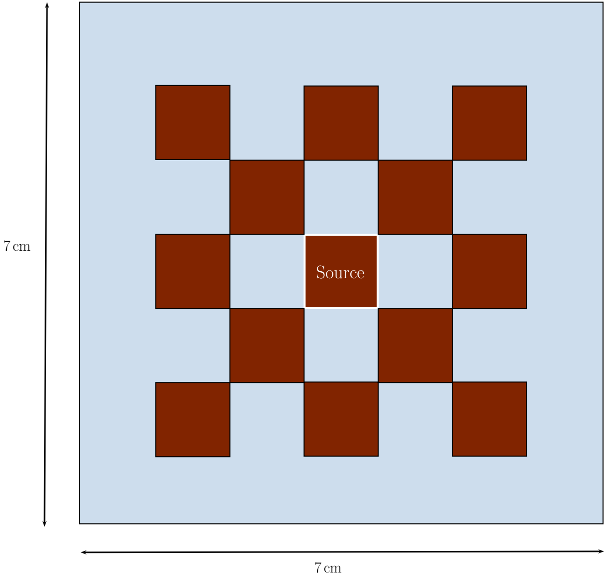

Figure: Schematic of the 2D Brunner lattice problem. The red region is a pure absorber (10 cm^{-1}), the blue region is pure scatter (1 cm^{-1}), with the the white bordered region a source.

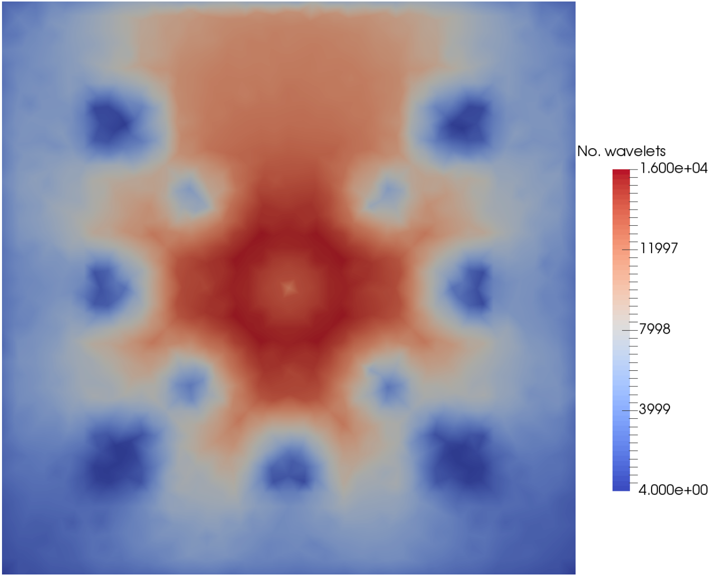

Figure: Number of angles applied with regular adaptivity after 7 adapt steps.

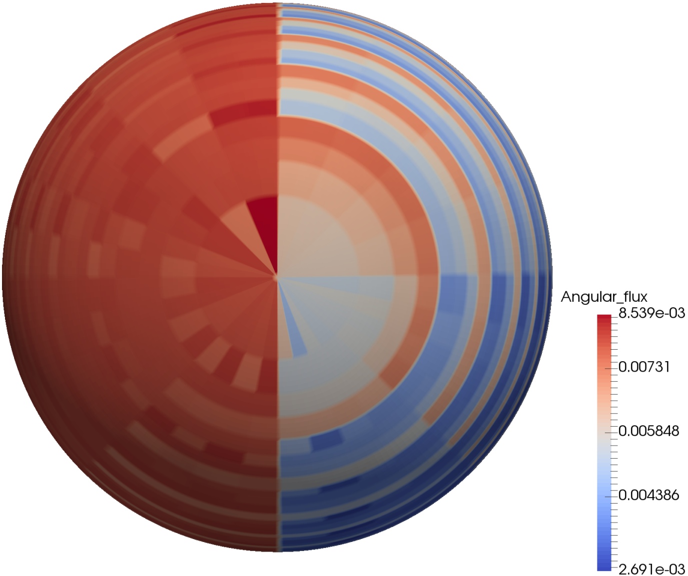

Figure: Adapted angular flux at $x = 3, y = 3.5$

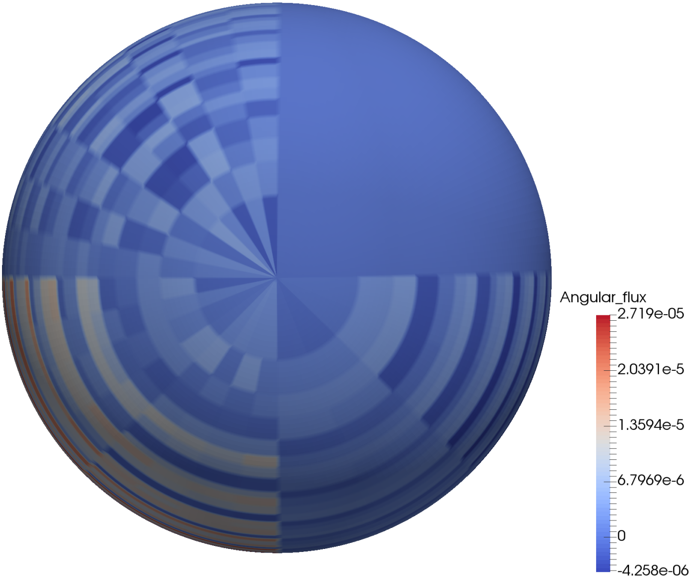

Figure: Adapted angular flux at $x = 2.5, y = 2.5$

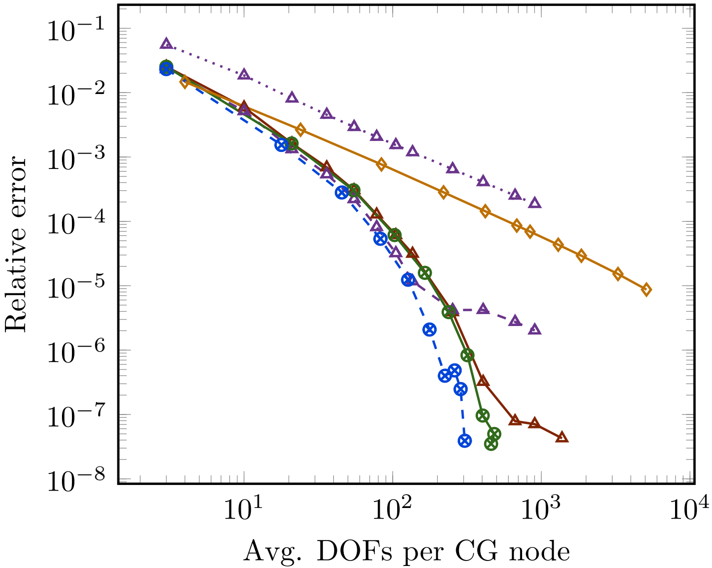

Figure: The ● are regular Haar adapts with threshold coefficient 1×10^{-5} with the dashed the standard Haar decomposition and the solid the non-standard. The △ is uniform P_n and ◇ is uniform P0-DG with level-set.

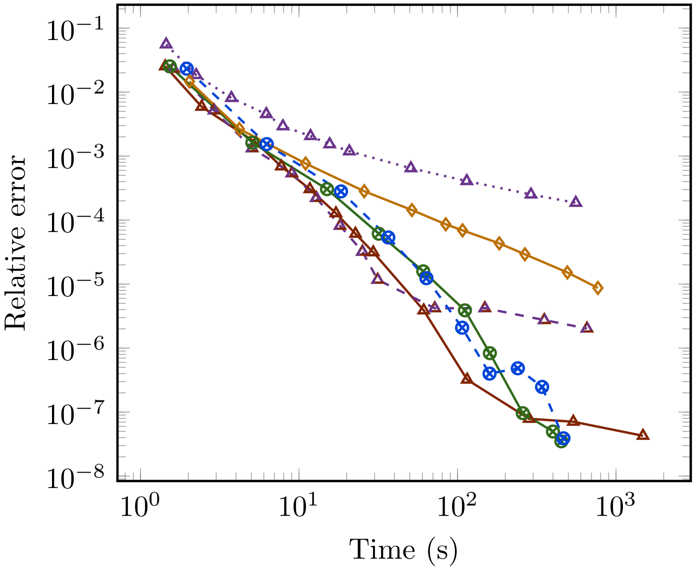

Figure: The ● are regular Haar adapts with threshold coefficient 1×10^{-5} with the dashed the standard Haar decomposition and the solid the non-standard. The △ is uniform P_n and ◇ is uniform P0-DG with level-set.

FETCH2 goal-based spatial adaptivity

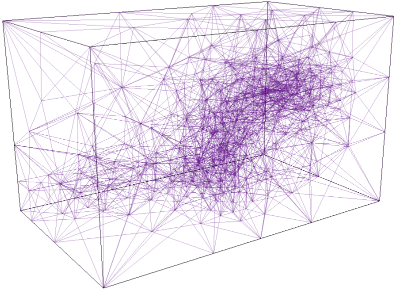

Figure: Initial mesh

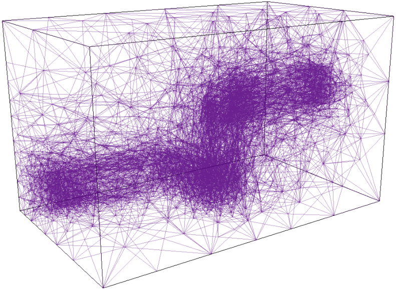

Figure: After one adapt

- Anisotropic hr spatial adaptivity is only refining the mesh where necessary to reduce error in the goal

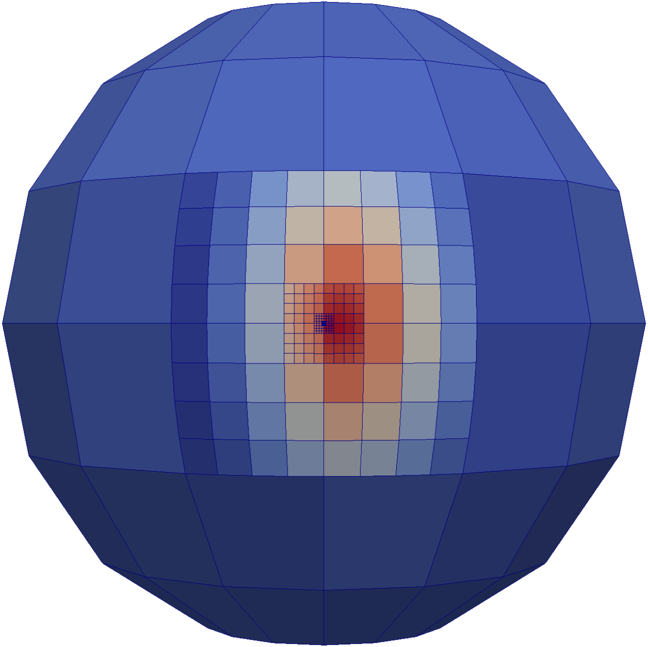

Figure: Angular adaptivity after 13 levels of refinement in a duct problem

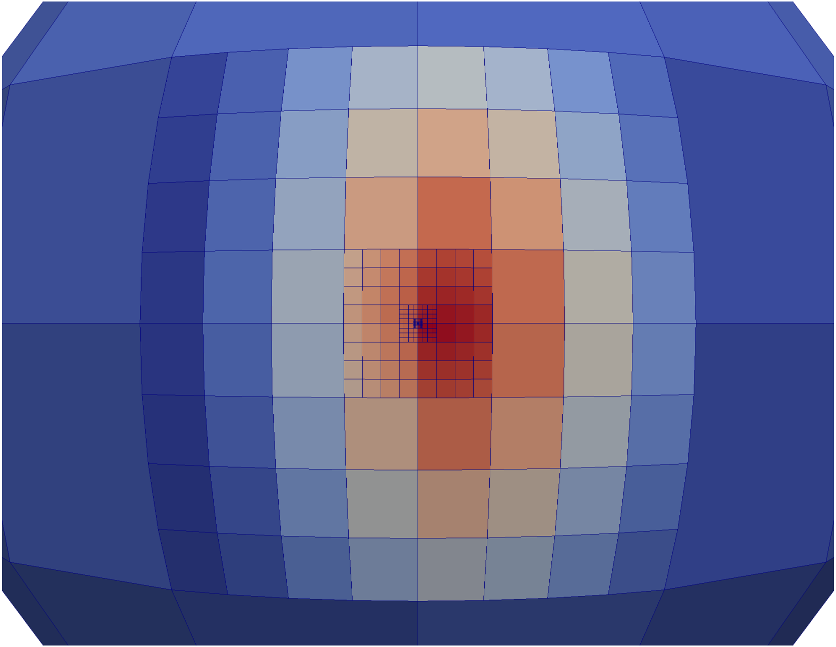

Figure: Angular adaptivity after 13 levels of refinement in a duct problem

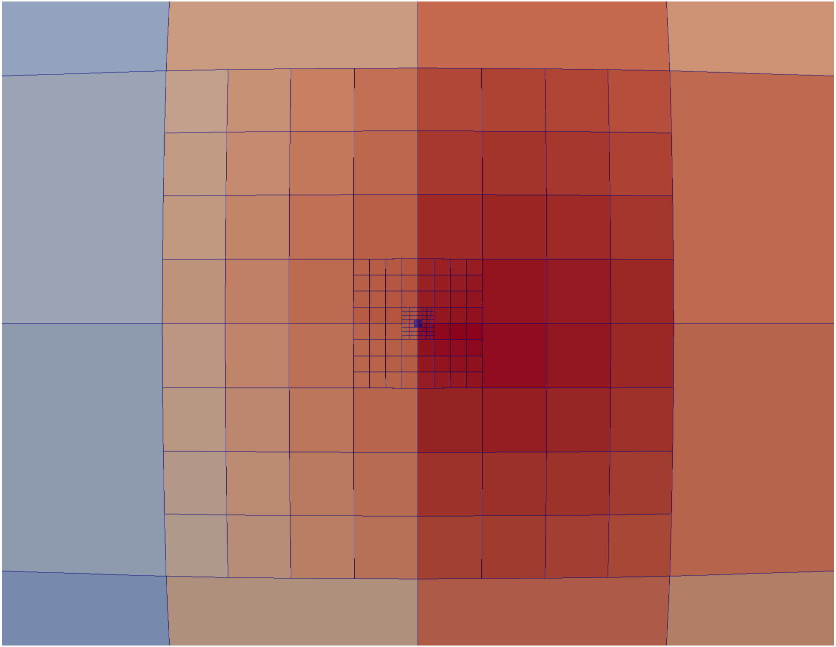

Figure: Angular adaptivity after 13 levels of refinement in a duct problem

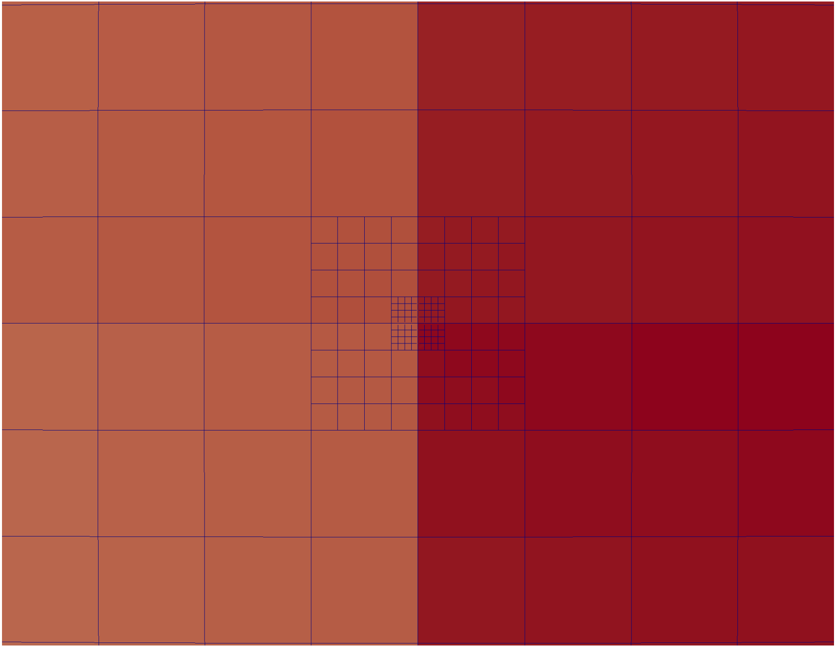

Figure: Smallest angular element - 9 $\times 10^{-8}$ sr